Eur. Phys. J. B **45**, 157–168 (2005)
DOI: 10.1140/epjb/e2005-00073-y

THE EUROPEAN PHYSICAL JOURNAL B

Epitaxial growth and magnetic exchange anisotropy in Fe_3O_4/NiO bilayers grown on MgO(001) and Al_2O_3(0001)

C. Gatel[1], E. Snoeck[1,a], V. Serin[1], and A.R. Fert[2]

[1] CEMES-CNRS, 29 rue J. Marvig, BP 94347, 31055 Toulouse Cedex, France
[2] LNMO, 135 avenue de Rangueil, 31077 Toulouse Cedex 4, France

Received 15 September 2004 / Received in final form 10 December 2004
Published online 15 March 2005 –

Abstract. Epitaxial Fe_3O_4/NiO bilayers were epitaxially grown on MgO(001) and Al_2O_3(0001) substrates to investigate the influence of the fully spin compensated (001) and the non-compensated (111) NiO interface planes between the ferromagnetic (F) and antiferromagnetic (AF) layers on the AF/F exchange coupling. Bilayers of different magnetite thicknesses and constant NiO thickness were investigated. The structural characterizations indicate a perfect epitaxy of the two layers for the both growth directions in the two Fe_3O_4/NiO/MgO(001) and NiO/Fe_3O_4/Al_2O_3(0001) systems. An epitaxial ferrimagnetic (Ni,Fe)Fe_2O_4 phase is observed at the AF/F interface when the NiO oxide is grown on the top of the Fe_3O_4 layer while a perfectly flat AF/F interface is observed in the Fe_3O_4/NiO/MgO(001) system exhibiting only a very slight interdiffusion. Magnetic measurements indicate a relative strong bias at 300 K for the bilayers grown on Al_2O_3(0001), which decreases with the inverse of the ferrimagnetic layer thickness as theoretically expected. On the contrary, a zero exchange biasing is observed at 300 K for the bilayers grown on MgO(001).

PACS. 61.16.-d Electron, ion, and scanning probe microscopy – 68.55.-a Thin film structure and morphology – 75.50.Ee Antiferromagnetics – 75.50.Gg Ferrimagnetics

1 Introduction

Understanding magnetic interactions between thin layers through their interface has become of considerable physical and technological interest for instance for the development of magnetoresistive (MR) devices. The direct exchange coupling between a ferromagnetic (F) layer and an antiferromagnetic layer (AF) is more and more studied nowadays because the pinning of the F layer has to be optimized in the spin valves used in MR head devices [1–3] and in the magnetic tunnel jonctions [4] developed for MRAM (Magnetic Random Access Memory) [5,6]. The pinning effect between an AF and a F layers generally induces an increase of the coercive field (H_c) of the F layer and a shift of its hysteresis loop by a so-called bias field (H_b). This behavior is noticed when the AF/F bilayer has been cooled through the ordering temperature of the AF (Néel temperature, T_N) under the application of a magnetic field.

The AF/F exchange coupling has been observed for the first time in 1957 by Meiklejohn and Bean [7–10] on fine Co particles. Similar coupling has been evidenced few years later on F films deposited on AF single crystals i.e. CoO [11,12] and NiO [13–16]. Growing a Ni layer on different polished surfaces of a NiO single crystal, Berkowitz and Greiner [16] have first demonstrated the role of the spin configuration of the NiO surface at the AF/F interface: compensated for NiO(001) or fully uncompensated for NiO(111).

The first model to describe the exchange coupling was proposed by Meiklejohn and Bean. It considers an AF/F interface formed by a rigid uncompensated AF surface where only one sublattice of spin is present. The direct coupling between the spins through the AF/F interface induces an additional unidirectional field responsible for the bias. This model predicts an exchange bias about 100 times stronger than the ones experimentally measured. In a more recent model Malozemoff assumes random exchange interactions between the interfacial spins of the F and AF layers through a rough AF/F interface [17,18]. In this model the roughness of the interface creates magnetic domains in the AF layer which are responsible for an exchange coupling even if the AF surface is spin compensated. The H_c and H_b values deduced from his model are close to the experimental results. In another model, Mauri [19] takes into account the rotation of the AF layer spins dragged by the magnetization switching of the F layer. This model implies the appearance of a planar domain wall parallel to the interface in the AF layer. H_b values deduced from this last model are also close to the experimental ones. More recently, micromagnetic calculations developed by Koon [20] for fully compensated interfaces have shown the stability of a so-called spin flop

[a] e-mail: snoeck@cemes.fr

state where the spins of the AF and F layers are perpendicularly oriented. In all these models the AF/F exchange coupling is an interface phenomenon for which both the bias field and the coercive field decrease with the inverse of the ferrimagnetic layer thickness.

As pointed by Nogues and Schuller in their review paper [21] much work has been dedicated to AF/F bilayers grown by various methods (MBE, sputtering and pulsed laser deposition). Most of the studies focus on the modifications of the magnetic behaviour of the F layer, generally the coercivity enhancement and a shift of the hysteresis loop because of their applications in spin electronic devices. The AF materials mostly studied are oxidized transition metals (NiO, CoO and FeO) and metallic films (PtMn, NiMn, FeMn) [22–24] because of their high T_N and good corrosion properties but also fluorides and nitrides materials (FeF_2, FeS) [25,26].

Experiments performed on ferromagnetic/AF bilayers have been extended to Ferrimagnetic/AF bilayers. Results published by Van der Zaag et al. [27,28] on [111] and [100] Fe_3O_4/CoO epitaxial bilayers do not evidence any drastic difference in the magnetic exchange for the two (111) and (100) types of AF/F interfaces. These observations disagree somehow with the expected influence of spin compensated and uncompensated surfaces as observed for instance, by Berkowitz and Greiner on the two Ni/NiO(100) and Ni/NiO(111) interfaces [16]. However, structural non homogeneities and/or roughness of the Fe_3O_4/CoO interfaces could be responsible for such discrepancy. In the continuity of these works, we concentrate our study on the exchange coupling in Fe_3O_4/NiO epitaxial bilayers focusing on the influence of the AF/F interfaces and on the thickness of the F layer. Our work is also motivated because of the half metallic property of Fe_3O_4 [29] which makes it of a great interest in spin electronic devices (magnetic spin filtering, tunnel junctions etc.). A first step of this work was to succeed in growing epitaxial Fe_3O_4 and NiO thin layers in two growth directions. Single Fe_3O_4(100) and (111) thin films, Fe_3O_4/NiO(111) and Fe_3O_4/NiO(100) bilayers have been successfully epitaxially grown on MgO(001) and Al_2O_3(0001) substrates. The exchange coupling is an interface phenomenon which is known to be very sensitive to many parameters, such as the magnetization of the F material, the thickness of layers, the AF/F crystallographic orientation relationship and other interface effects like interdiffusion, roughness, interface phases precipitation... A first part of this work is then dedicated to the analysis of crystallographic characteristics of the bilayers. The role of the Fe_3O_4/NiO interface roughness and geometrical imperfections are accurately investigated since the interface planeity is even more crucial in case of ferrites, where the Fe cations are located in two sites antiferromagnetically coupled.

A second part of this work is devoted to the investigation of the Fe_3O_4/NiO exchange coupling. We focus our study on the changes of the coercitive field and the bias as a function of the AF/F interface planes and the thickness of the ferromagnetic layer.

2 Materials and experimental procedure

The magnetite (Fe_3O_4) is an attractive ferrimagnetic material because of its high Curie temperature (860 K) and its predicted half metallic electronic structure. It has been intensively studied this last decade [29–38] both in thin films and bulk. The magnetite has an inverse spinel fcc structure (Fd-3m) with a lattice parameter of $a = 0.8397$ nm at 300 K. That complex AB_2O_3 structure contains 8 Fe_3O_4/unit cell, one third of the Fe cations are Fe^{2+} located in the B octahedral sites, and the two other thirds are Fe^{3+}, half of them being on the octahedral B sites and the others on the tetrahedral A sites. The interaction between the A and B sites is antiferromagnetic leading to a saturation moment per formula unit close to 4 μ_B (480 emu/cm^3). The bulk ferrimagnetic oxide has a low magnetic anisotropy with a coercive field of about 310 Oe [36] at room temperature (RT) and ranging between 1000 to 1200 Oe at 20 K. A phase transition occurs at the so-called Verwey temperature, $T_V = 120$ K i.e. below T_V, the magnetite adopts a monoclinic structure, becomes insulting and its magnetic susceptibility changes.

NiO is widely studied as it is an antiferromagnetic ionic insulator with a high thermal stability and a good resistance to corrosion. Its Néel temperature is $T_N = 523$ K. It adopts a rocksalt structure with a lattice parameter equal to 0.418 nm. In this fcc arrangement, O^{2-} and Ni^{2+} ion planes alternate along the $\langle 111 \rangle$ direction. The magnetic moments held by Ni ions, are ferromagnetically arrayed within a $\{111\}$ sheet. Successive $\{111\}$ planes are coupled antiparallely. In a given $\{111\}$ plane, the spin lies along a $\langle 110 \rangle$ direction. Thus the NiO$\{001\}$ plane are spin compensated surfaces while NiO$\{111\}$ is a polar surface with a magnetic moment [39] (Fig. 1). The parameter of the magnetite is two times larger than the one of NiO. Considering half of a magnetite cell, the lattice misfit between the two oxides is less than one percent (0.4%).

MgO is isostructural to NiO with a lattice parameter slightly larger and equal to 0.421 nm. The misfit between NiO and MgO (resp. Fe_3O_4 and MgO) is about 0.7% (resp. 0.3%).

Al_2O_3 has a corrindon structure (Fd-3m) with the parameters $a = 0.475$ nm and $c = 1.2989$ nm. When deposited on Al_2O_3(0001) surface the misfit between the magnetite and the sapphire is equal to 8%.

The oxide layers were grown in an Plassys ultra high vacuum (UHV) chamber whose base pressure is 2×10^{-8} mbar. The 10 mm $\times$ 10 mm MgO and Al_2O_3 substrates were annealed at 800 °C for an hour before deposition. NiO was shown to epitaxially grow with the expected stoechiometry at temperature no less than 700 °C [40–42]. It has then been grown at 700 °C using two NiO facing targets under 10% O_2 partial pressure while the Fe_3O_4 layers were grown at 400 °C by means of two Fe_2O_3 facing targets, both were sputtered with a RF power of 100 W. The Ar plasma pressure was kept at 5×10^{-3} mbar during deposition. The UHV chamber is fitted with an electron gun (20 kV) to perform Reflection High Energy Electron Diffraction (RHEED) experiments. The flatness and the crystalline quality of the substrate and layers surfaces were

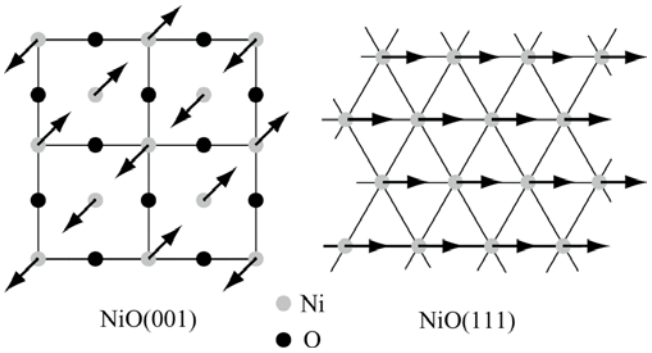

Fig. 1. Sketch of the NiO surfaces showing the spin-compensated (001) surface and the spin uncompensated (111) surface.

checked by RHEED measurements at the end of the annealing step and after the growth of each layer.

Fe_3O_4 and NiO were expected to grow in the [001] and [111] direction when they are deposited on MgO(001) and Al_2O_3(0001) surfaces respectively. NiO was shown to create very rough surface when growing in the ⟨111⟩ direction [42]. Thus to get flat F/AF (111) and (001) interfaces, two types of bilayers were prepared: (NiO/Fe_3O_4) deposited on Al_2O_3(0001) and (Fe_3O_4/NiO) grown on MgO(001). Moreover, to check the influence of the stacking order on the magnetic properties another batch of sample was grown on MgO(001) inverting the two oxide layers i.e.: NiO/Fe_3O_4/MgO(001). To force an uniaxial magnetic axis, the bilayers were cooled down in-situ through the Néel temperature of the nickel oxide under an magnetic field of 650 Oe applied along the NiO [100] direction for bilayers grown on MgO[001] and along NiO [110] for the ones deposited on Al_2O_3(0001).

The structure of the layers and the quality of the NiO/Fe_3O_4 interfaces were investigated by X-ray diffraction and Transmission Electron Microscopy (TEM) experiments. X-ray diffraction analyses were performed using a Seifert four circle high-resolution diffractometer with a Cu-Kα radiation (0.15406 nm) and a beam divergence of 0.1°. The TEM experiments were performed in conventional and in high resolution mode (HRTEM) using a CM30/ST microscope whose point resolution is 0.19 nm. Electron Energy Loss Spectroscopy (EELS) were also performed on CM20 ST microscope equipped with a Gatan PEELS spectrometer with an energy resolution of 1.2 eV. EELS analyses were carried out doing line scan across the interface in STEM mode with a probe size of 2.5 nm. For TEM studies, cross-sectional and plane view specimens were thinned by mechanical grinding and ion-milling (using a PIPS system) to achieve the electron transparency.

Magnetic properties were investigated at RT and at 20 K using a SQUID magnetometer "Quantum Device". A magnetic field of $\pm 10^4$ Oe was applied parallel to the common easy axis defined during the cooling after deposition. The first hysteresis loop was measured at room temperature, then the sample is cooled down to 20 K under a magnetic field of 10^4 Oe and a second hysteresis loop was measured at low temperature.

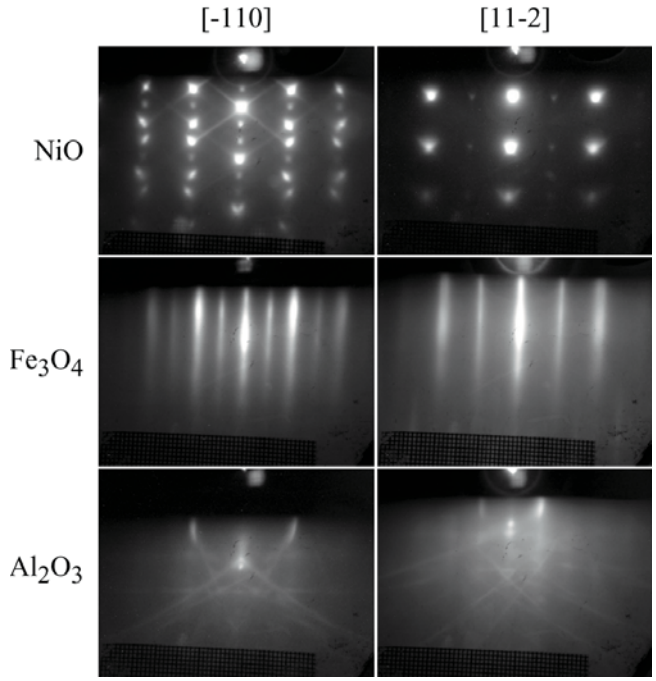

Fig. 2. RHEED pattern obtained on the NiO/Fe_3O_4 bilayer grown on Al_2O_3(0001).

3 Epitaxial growth and structural properties of the (NiO/Fe_3O_4) bilayers deposited on Al_2O_3(0001) and MgO(001)

3.1 (NiO/Fe_3O_4) bilayers grown on Al_2O_3(0001)

Five (NiO/Fe_3O_4) bilayers with thickness of magnetite of 5, 10, 20, 35 and 50 nm and a constant NiO thickness of 66 nm have been deposited on Al_2O_3(0001). The magnetite was first grown at 400 °C then the temperature was raised up to 700 °C and the NiO layer was deposited. RHEED experiments were performed at each step of the growth i.e. on the substrate surface, after the NiO deposition and at the end of the whole bilayer growth (Fig. 2). In that figure, the sharp and elongated RHEED reflections evidence the flat Al_2O_3(0001) surface and the 2D epitaxial growth of the Fe_3O_4 layer while the spots observed on the NiO layer demonstrate a 3D rough surface. In previous works, Warot et al. [42] have shown that when growing NiO in the ⟨111⟩ direction, the weakest value of the surface energy of the {100} planes results in an extremely rough surface constituted by tetrahedral islands with {100} type facets. This is in agreement with the high roughness of the top NiO surface observed in the RHEED pattern in Figure 2. X-Ray reflectivity experiments in Figure 3 confirm these observations and show flat Fe_3O_4/Al_2O_3 and NiO/Fe_3O_4 interfaces with a roughness of about 0.35 nm and a rough top NiO surface. Symmetrical $\Theta-2\Theta$ X-Ray diffraction experiments evidence

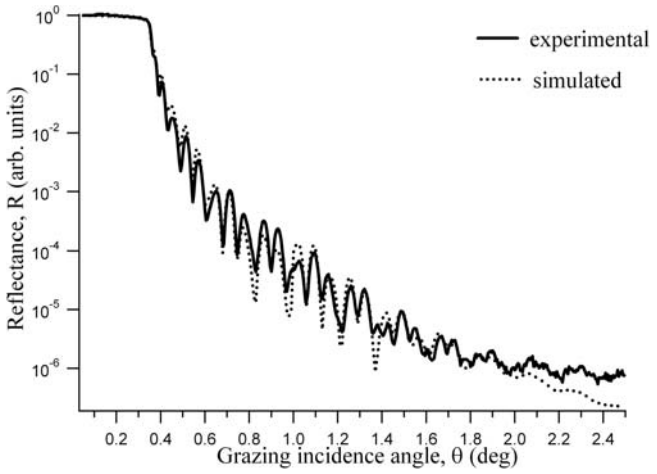

Fig. 3. X-Ray reflectivity spectra of (NiO – 66 nm/Fe_3O_4 – 30 nm) bilayer grown on Al_2O_3(0001).

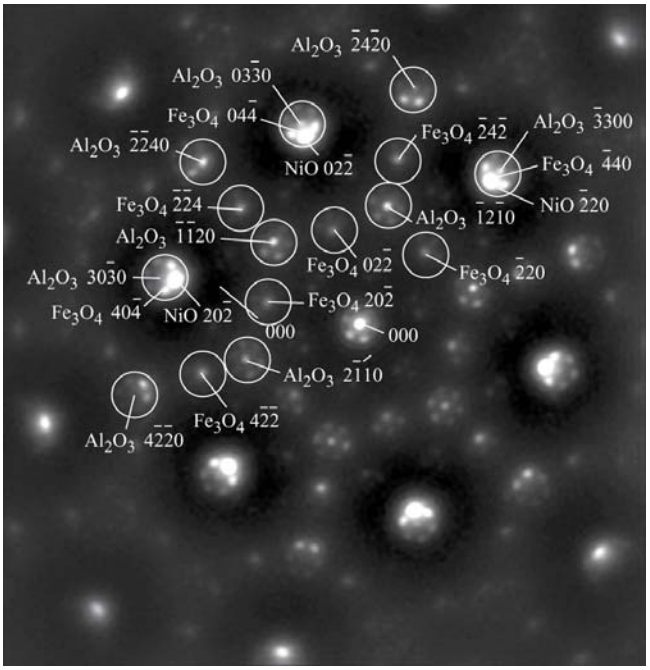

Fig. 4. Plane view SAED pattern of a (NiO – 66 nm/Fe_3O_4 – 30 nm) bilayer grown on Al_2O_3(0001).

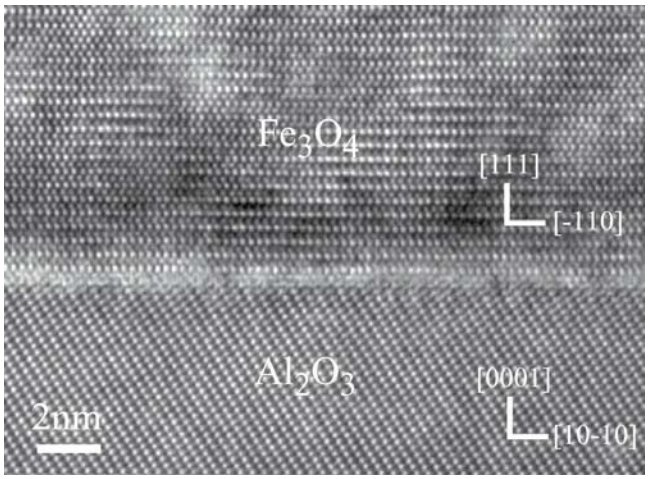

Fig. 5. HRTEM micrograph of the interface between Fe_3O_4 and Al_2O_3(0001) studied along the [−110] zone axis.

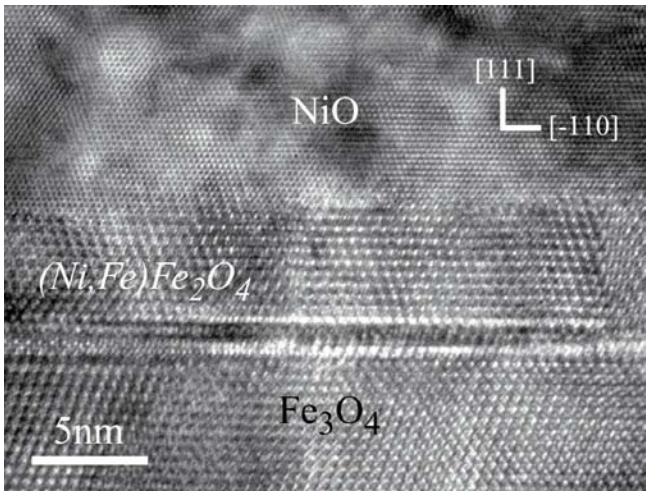

Fig. 6. HRTEM micrograph of the AF/F interface in (Fe_3O_4/NiO) bilayer grown on Al_2O_3(0001) and studied along the [11-2] zone axis.

the 0006 peak of Al_2O_3 (d = 0.2165 nm) and the 111 reflections of the NiO and Fe_3O_4 fcc structure (respectively d_{111} = 0.2413 nm and d_{222} = 0.2424 nm). It demonstrates the [111] growth direction of the bilayer deposited on Al_2O_3(0001) which keeps the 6-fold symmetry of the surface substrate. No evidence of residual strain of the magnetic layers was evidenced within the accuracy of the X-ray diffraction measurements.

TEM analyses (HRTEM and EELS) were carried out to study the structure of each layer, their orientation relationships and the structural qualities of the interfaces. A Selected Area Electron Diffraction (SAED) pattern obtain on a plane view sample i.e. studied in a direction parallel to the growth direction is reported in Figure 4. On the latter are reported the reflection indices corresponding to the different layers and the substrate. The satellite reflections appearing around the main reflections confirm the good epitaxy of the whole system. The orientation relationships deduced from such a SAED pattern are: NiO(111) [2-20] // Fe_3O_4 (111) [4-40] // Al_2O_3(0001) [30-30].

In Figure 5 is reported a cross section HRTEM micrograph of the Fe_3O_4/Al_2O_3 interface in the Fe_3O_4 – 15 nm thick sample studied along the [11 − 2] zone axis. The interface appears perfectly flat without any noticeable interface phase at the atomic scale. Similar HRTEM studies were performed on the NiO/Fe_3O_4 interfaces as reported in the cross-sectional micrograph in Figure 6 obtained on a bilayer studied along the [–110] zone axis. The appearance in the magnetite film of a disturbed layer running parallel to the NiO/Fe_3O_4 interface at about 3 to 5 nm below it is evidenced. This default was found in all of the [111] bilayers at the NiO/Fe_3O_4 interfaces. The HRTEM contrasts observed between this defect and the NiO/Fe_3O_4 interface

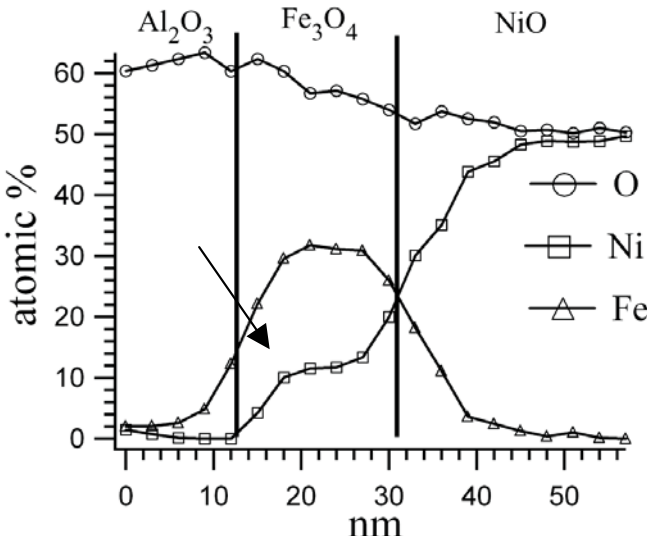

Fig. 7. Chemical profile deduced from EELS experiments performed on a (NiO – 66nm/Fe_3O_4 – 15 nm) bilayer grown on Al_2O_3(0001). The arrow indicates a bump in the Ni profile associated the (Ni,Fe)Fe_2O_4 interface phase.

are similar to those of the magnetite. EELS measurements have been performed doing a line scan profile along the growth direction. The Fe and Ni composition profiles reported in Figure 7 were deduced from the EELS scans. The bump in the Ni profiles (arrowed in the figure) confirms the appearance of a secondary phase at the NiO/Fe_3O_4 interface. The HRTEM contrast and the increase in the Ni content in that area suggest that it is a non stoechiometric nickel ferrite: (Ni,Fe)Fe_2O_4 spinel. The temperature at which the NiO is deposited (700 °C) is supposed to be responsible for an important diffusion of the Ni in the magnetite resulting in the formation of the nickel ferrite phase. As observed in the HRTEM micrograph in Figure 6, the interface between this nickel ferrite intermediate phase and NiO is however fairly flat. This is in agreement with the X-ray reflectivity measurements which cannot separate the pure magnetite phase from the (Ni,Fe)Fe_2O_4 spinel one and indicates a AF/F interface roughness of 0.35 nm. We then assume that the NiO layer is almost stoechiometric and that the mixed layer presents a composition change from an highly nickel doped region close to the NiO interface to a pure Fe_3O_4 phase at about 5 nm inside the ferrite layer. The thickness of this mixed phase was not found to vary with the thickness of the magnetite layer.

3.2 (NiO/Fe_3O_4) bilayers grown on MgO(001)

Bilayers with various magnetite thicknesses and a constant NiO thickness of 66 nm were deposited on MgO(001) and two batches of samples were grown inverting the order of the AF/F sequence.

3.2.1 Fe_3O_4 (t)/NiO – 66 nm/MgO(001)

In that set of samples, the NiO oxide was first deposited at 800 °C under a partial pressure of oxygen, afterwards

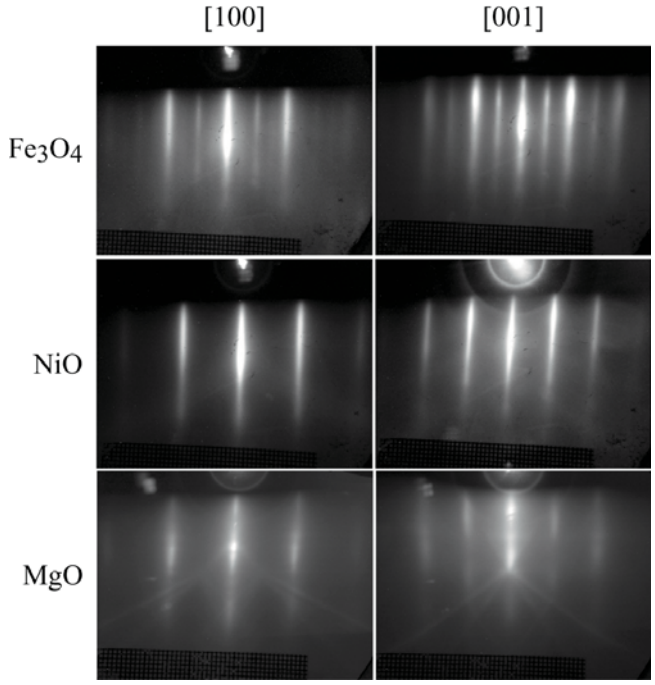

Fig. 8. RHEED pattern obtained on the Fe_3O_4/NiO bilayer grown on MgO(001).

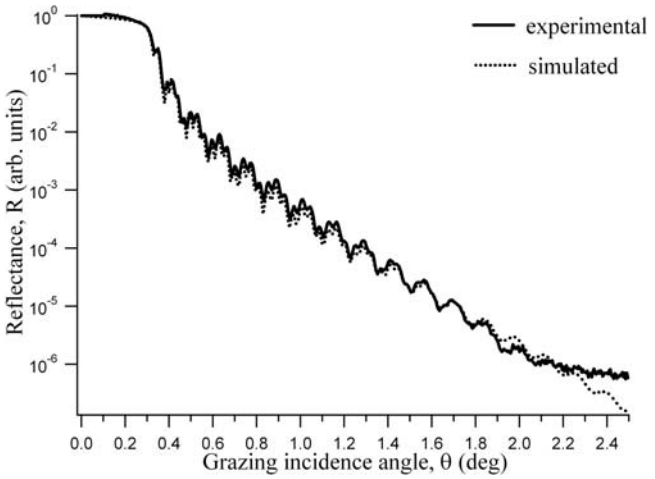

Fig. 9. X-Ray reflectivity spectra of (Fe_3O_4 – 30 nm/NiO – 66 nm) bilayer grown on MgO(001).

the sample was cooled down to 400 °C and the magnetite layer was grown. Six different magnetite thicknesses i.e. 5, 10, 20, 30, 50, 100 nm, have been deposited. In agreement with previous results [29,30] RHEED patterns in Figure 8 indicate a 2D growth of the NiO layer on MgO(001) with a cube on cube epitaxial relation and a flat surface. Similar epitaxial 2D growth was obtained when deposited Fe_3O_4 on NiO(001). X-ray reflectivity experiments confirm the flatness of each interface (Fig. 9). They indicate a mean roughness of 1.1 nm for the NiO/MgO interface, of 0.7 nm for the Fe_3O_4/NiO one and of 0.6 nm for the top Fe_3O_4(001) surface. X-Ray diffraction experiments confirm the [001] growth of the bilayers i.e. the 004 peak

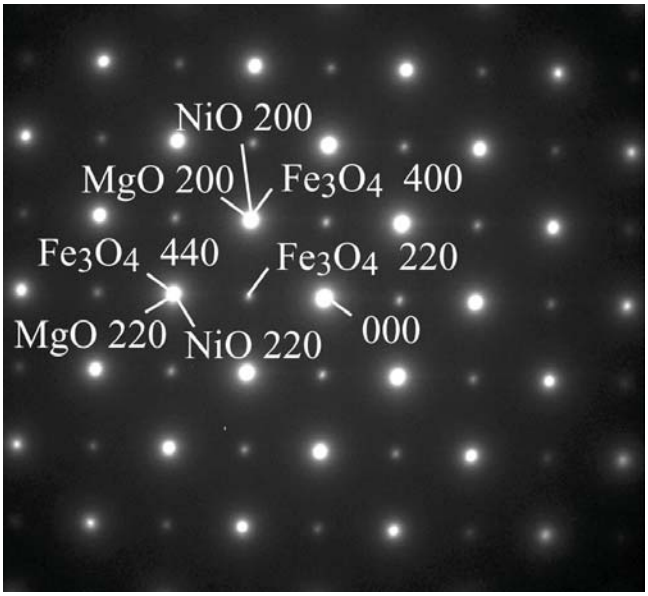

Fig. 10. Plane view SAED pattern of a (Fe_3O_4 – 20 nm/NiO – 66 nm) bilayer grown on MgO(001).

of the magnetite and the 002 one of NiO are observed in the symmetrical Θ–2Θ scans together with the 002 reflection of the MgO substrate. Their positions correspond to the expected out-off plane lattice distance for the unstrained material (within the experimental error): $d_{002\text{-NiO}} = 0.209$ nm, $d_{004\text{-}Fe_3O_4} = 0.21$ nm. TEM experiments were performed to analyse the structure of both layers and study the quality of the NiO/MgO(001) and the Fe_3O_4/NiO(001) interfaces. A SAED pattern obtained in plane view sample is reported in Figure 10. On the latter are indexed the reflections belonging to the Fe_3O_4 and NiO layers and to the MgO substrate. The reflections due to NiO and MgO cannot be separated since the lattice parameter of the two isostructural compounds are too close. As for the [111] growth direction, the SAED pattern clearly evidence the high quality of the epitaxial growth of the whole system whose epitaxial relationships are: Fe_3O_4(001)[110] // NiO(001)[110] // MgO(001)[110].

HRTEM analyses were performed to locally study the quality of all the interfaces. Similar results as the one obtained by Warot et al. [29,30] were observed on the NiO/MgO(001) interface. In Figure 11 is reported an HRTEM micrograph of a Fe_3O_4/NiO(001) interface studied along the [100] zone axis. The epitaxial growth is confirmed and a perfectly flat interface is obtained without any evidence of an interface phase appearance. EELS measurements have been performed doing a line scan profile along the growth direction. The composition profiles reported in Figure 12 were deduced from the EELS scans. It indicates a very slight interdiffusion of Ni and Fe. It then should also exist a non stoechiometric (Ni,Fe)Fe_2O_4 phase near the interface but with much less Ni content than what is observed in the bilayers grown on the Al_2O_3(0001) substrate.

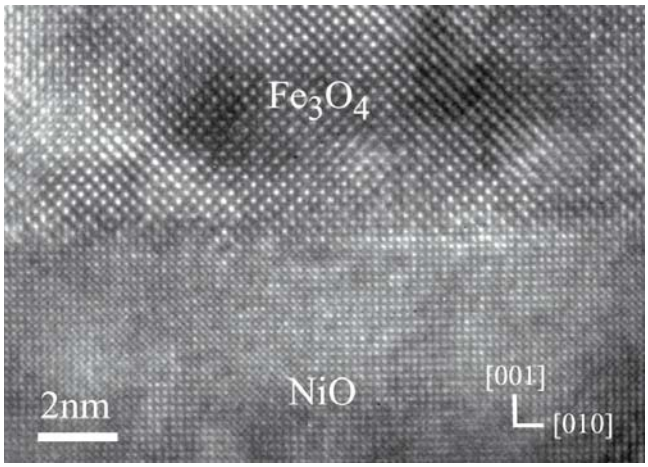

Fig. 11. HRTEM micrograph of an F/AF interface in a Fe_3O_4/NiO bilayer grown on MgO(001) studied along the [100] zone axis.

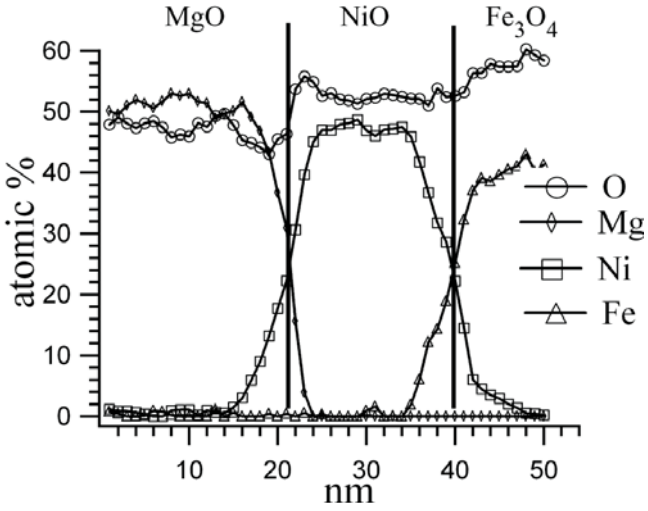

Fig. 12. Chemical profile deduced from EELS experiments performed on a (Fe_3O_4–20 nm/NiO – 66 nm) bilayer grown on MgO(001).

3.2.2 NiO – 66 nm/Fe_3O_4 (t)/MgO(001)

To check the influence of the stacking sequence on the magnetic properties another batch of bilayers was grown on MgO(001) inverting the Fe_3O_4/NiO order i.e. the magnetite was first grown at 400 °C on the MgO(001) substrate then NiO was deposited at the top of the Fe_3O_4 layer at 800 °C. Five bilayers with magnetite thicknesses of 5, 10, 20, 35 and 50 nm and a constant 66 nm thick NiO layer have been grown. RHEED (Fig. 13) and X-ray experiments indicate that the [001] epitaxial growth of the Fe_3O_4 and NiO layers is also achieved without residual strain. In Figure 14 is reported an HRTEM micrograph of the NiO/Fe_3O_4 interface studied along the [100] zone axis. On the latter, an important roughness is evidenced with small (011) and (0-11) facets tilted by 45° of the Fe_3O_4(001) surface. It suggests that, after the annealing step at 800 °C, the surface becomes rough. We assume

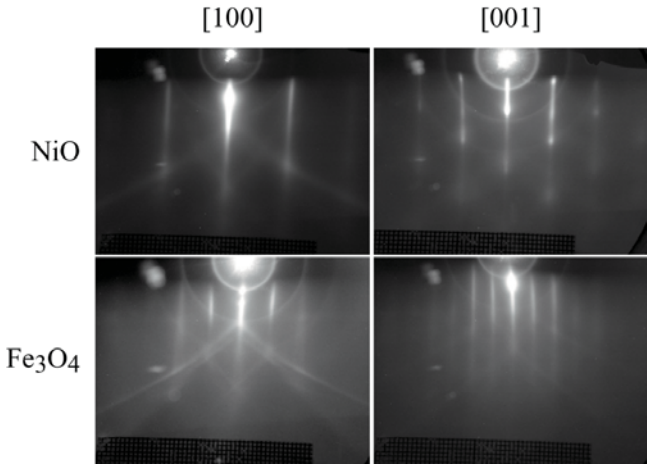

Fig. 13. RHEED pattern obtained on the NiO/Fe_3O_4 bilayer grown on MgO(001).

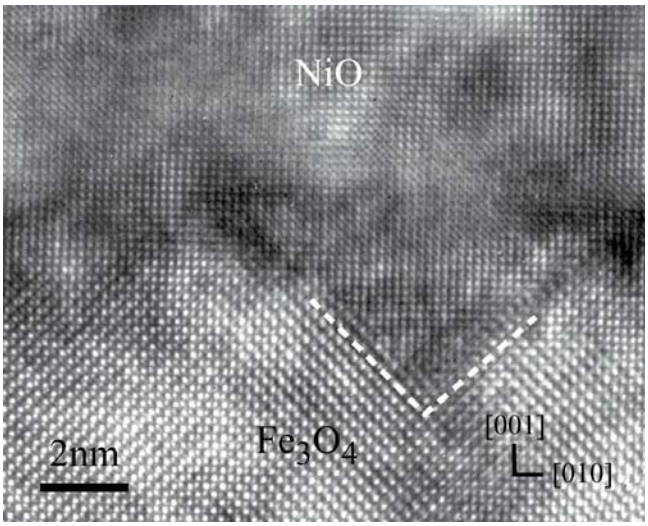

Fig. 14. HRTEM micrograph of an F/AF interface in a NiO/Fe_3O_4 bilayer grown on MgO(001) studied along the [100] zone axis.

these facets appear during the NiO growth because they were not observed in single Fe_3O_4 layer. As obtained in NiO/Fe_3O_4 bilayers grown on $Al_2O_3(0001)$, the high temperature deposition of NiO (800 °C) is believed to be responsible for an important interdiffusion between NiO and Fe_3O_4 leading to a rough interface and to the appearance of a possible $(Ni,Fe)Fe_2O_4$ interface phase.

4 Magnetic properties

4.1 (NiO/Fe_3O_4) bilayers grown on $Al_2O_3(0001)$

SQUID measurements were first performed on a single Fe_3O_4 layer epitaxially grown on $Al_2O_3(0001)$ substrate. The Figure 15 presents the hysteresis loops at 20 K obtained on a 20 nm thick Fe_3O_4 single layer and on a bilayer with the same Fe_3O_4 thickness coupled to a 66 nm thick NiO layer.

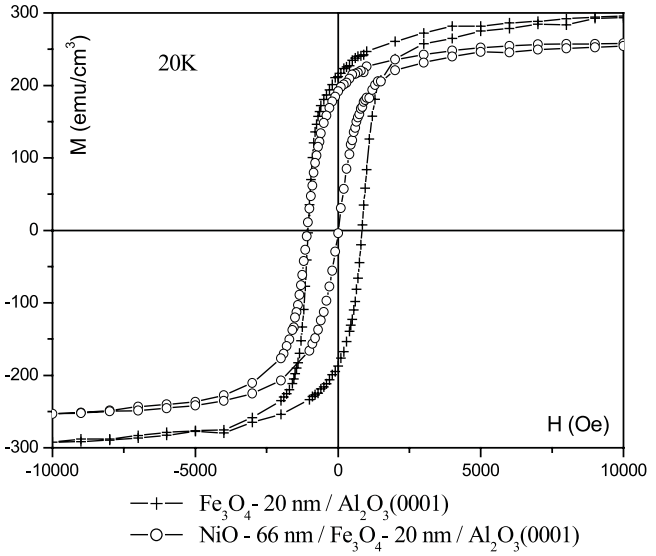

Fig. 15. SQUID measurements of the hysteresis loops at 20 K of a 20 nm thick Fe_3O_4 single layer and NiO-66nm/Fe_3O_4 – 20 nm bilayer grown on $Al_2O_3(0001)$.

The coercive field of the single Fe_3O_4 layer is about 300 Oe at RT and 1000 Oe at 20 K. These H_c values are in the range of those published in the literature. As observed in many others studies of magnetite thin films [38], the saturation of the magnetization is not reached in a 1 tesla applied field since we obtained 2.2 μ_B per formula unit which is significantly lower than the bulk value (4.1 μ_B). The magnetic moment measured at 1 tesla increases with the magnetite thickness i.e. 3 μ_B and 3.4 μ_B for magnetite layers of 30 nm and 50 nm respectively. This behaviour is commonly described as the result of antiphase boundaries (APBs) which locally reduces the magnetization [35,36]. This was recently confirmed by J.B. Moussy et al. who have shown that when the Fe_3O_4 thickness increases, the APB density decreases and the magnetization saturation rises up to its bulk value [38]. These APBs were always observed in all of our samples.

Due to the AF/F exchange coupling, the hysteresis loop of the NiO/Fe_3O_4 – 20 nm/$Al_2O_3(0001)$ system reported in Figure 15 is shifted by a bias field (H_b). The H_c value of the bilayer and its magnetization at 1 tesla are however less than the ones of the single magnetite layer of the same thickness. Similar hysteresis loops were measured at RT and 20 K for the five $NiO/Fe_3O_4/Al_2O_3(0001)$ bilayers with magnetite thickness of 5, 10, 20, 35 and 50 nm and a constant NiO thickness of 66 nm. Saturated magnetization moment, coercive field and bias field were extracted from these loops. The variations of H_c and H_b as a function of magnetite thickness were reported in Figure 16. Both curves exhibit the same behavior. Apart from the thinnest magnetite layer sample, H_c and H_b decrease with the inverse of the magnetite thickness with values larger at 20 K than at room temperature. This "$1/t$" dependence is the expected behavior for an exchange coupling mainly located at the AF/F interface as it is deduced from all models (Meiklejohn and Bean,

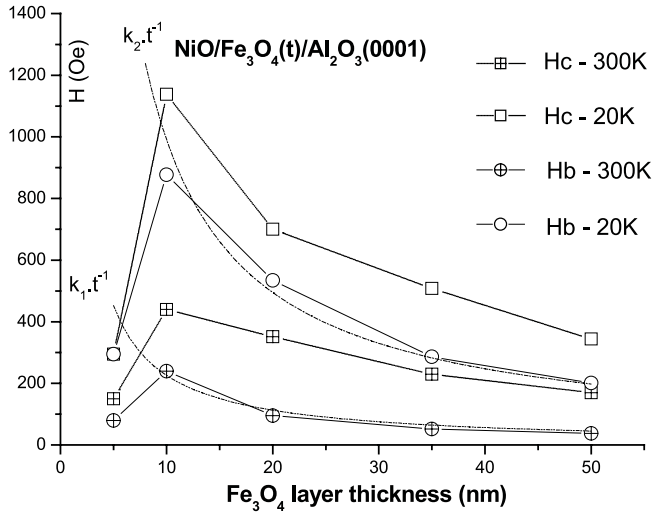

Fig. 16. Variations of H_c and H_b at 20 K and 300 K as a function of the magnetite thickness for (NiO/Fe_3O_4) bilayers grown on $Al_2O_3(0001)$ – in dashed line is the "$1/t$ fit" of the H_c and H_b decays.

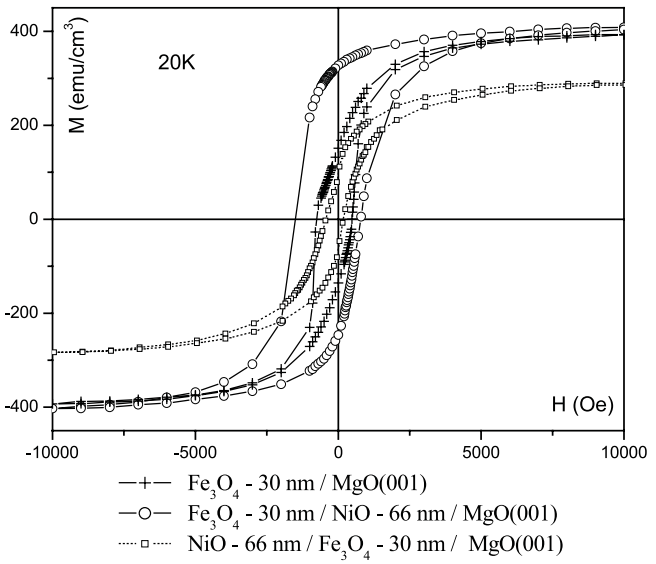

Fig. 17. SQUID measurements of the hysteresis loops at 20 K of a 20 nm thick Fe_3O_4 single layer and two (Fe_3O_4 – 30 nm/NiO – 66 nm) and (NiO – 66 nm/Fe_3O_4 – 30 nm) bilayers grown on MgO(001).

Malozemoff...) [7–10,17–20]. The exchange field and coercive field are maximum for a magnetite thickness of 10 nm (H_b = 850 Oe at 20 K and 250 Oe at RT, H_c = 1140 Oe at 20 K and 440 Oe at RT). The bias remains significant in the 50 nm thicker bilayer (250 Oe at 20 K and 50 Oe at RT) while the coercive field decreases to a value less than the one of the single layer. The weak values of H_b in thinnest magnetite layer sample (5 nm) can be interpreted facing to the structural results which indicate the appearance of a (Ni,Fe)Fe_2O_4 phase at the NiO/Fe_3O_4. In that thinnest sample, almost all the expected magnetite layer is formed by the intermixing (Ni,Fe) oxide. Since pure nickel ferrite, $NiFe_2O_4$, presents a slight weaker H_c and weaker saturated moment than the magnetite one (H_c =∼750 Oe at 4 K and ∼250 Oe at RT with a saturated moment equal to 2 μ_B), the exchange coupling between NiO and a non-stoechiometric (Ni,Fe)Fe_2O_4 is probably responsible for the weaker H_c field compared to the one expected with equivalent thickness of pure magnetite (Fig. 16).

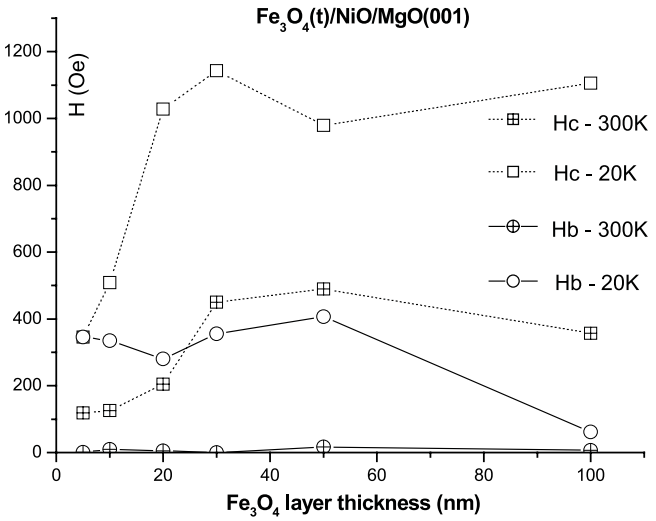

Fig. 18. Variations of H_c and H_b at 20 K and 300 K as a function of the magnetite thickness for (Fe_3O_4 (t)/NiO) bilayers grown on MgO(001).

4.2 NiO/Fe_3O_4 bilayers grown on MgO(001)

Analogous magnetic measurements have been performed on a 30 nm thick single Fe_3O_4 layer and on the (Fe_3O_4/NiO) and (NiO/Fe_3O_4) bilayers grown on MgO(001). The hysteresis loops obtained at 20 K on theses systems are reported in Figure 17. The coercive field of the single Fe_3O_4 layer grown on MgO(001) is about 250 Oe at 300 K and 700 Oe at 20 K, and its magnetization moment per formula unit is close to 3 μ_B at 1 tesla. The F/AF bilayer with the same Fe_3O_4 thickness displays the same saturated magnetization value while it is lower for the AF/F bilayer. The H_c and H_b variations as a function of the magnetite thickness in the F/AF deposited on MgO(001) are reported on the graph in Figure 18. These plots show a significant different behaviour than the one observed for bilayers grown on $Al_2O_3(0001)$. The bias field is nearly zero at RT whatever the magnetite thickness. At 20 K, it is almost constant and equal to ∼350 Oe up to a magnetite thickness of 50 nm then it vanishes for the bilayer with the thickest magnetite layer (100 nm). We have not observed the "$1/t$" dependence expected from all models [7–14]. The hysteresis loop of the F/AF bilayers shows a slight increase of the coercive field at 20 K (H_c = 1150 Oe). For measurements at RT, the coercive field first increases with the magnetite thickness and reaches its bulk values for a 20 nm to 30 nm thick magnetite layer. It then remains constant when increasing further the ferromagnetic thickness. At 20 K, the behaviour

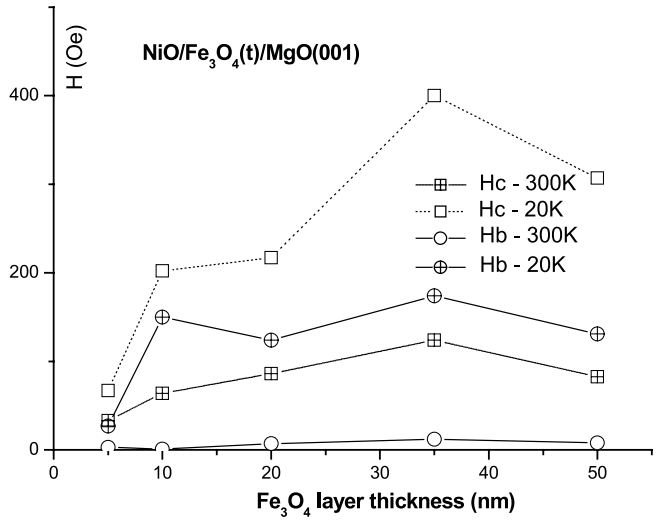

Fig. 19. Variations of H_c and H_b at 20 K and 300 K as a function of the magnetite thickness for (NiO/Fe_3O_4 (t)) bilayers grown on MgO(001).

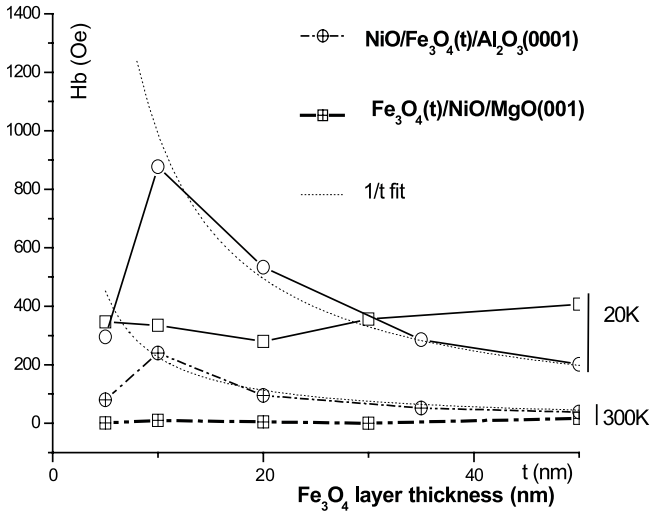

Fig. 20. Comparison between variations of H_b as a function of the magnetite thickness for (NiO/Fe_3O_4) bilayers grown on Al_2O_3(0001) and (Fe_3O_4/NiO) bilayers grown on MgO(001).

is the same but with a slight increase of the coercitive value compared with the bulk value ($H_c = 1150$ Oe).

In order to check whether such large difference in the magnetic behaviour could come from the order of the stacking sequence and the interface quality, similar experiments were carried out on five bilayers inverting the NiO and Fe_3O_4 stacking sequence. The magnetization at 1 tesla is less than the one of the single layer with the same thickness ($Ms \sim 2\ \mu_B$). The H_c and H_b evolutions as a function of the magnetite thickness in the system: NiO – 66 nm/Fe_3O_4 (t)/MgO(001) are reported in Figure 19. The bias is almost constant with the magnetite thickness, equal to zero at RT and ∼150 Oe at 20 K establishing the subsistence of an exchange coupling at this temperature. The coercive field slightly increases with magnetite thickness to reach a constant value far below the one obtained in the previous samples. We assume that this bias, weaker in the AF/F bilayers than the one measured on the F/AF bilayers deposited on MgO(001), is due to the rough interface and the interdiffusion between Ni and Fe.

5 Discussion

One of the most exciting aim of this study was to observe eventual distinct magnetic behaviour for the two series of samples $NiO/Fe_3O_4/Al_2O_3$(0001) and Fe_3O_4/NiO/MgO(001) resulting from different interfaces with respectively [111] and [100] oriented epitaxial NiO antiferromagnetic layer. The series NiO/Fe_3O_4/MgO(001) could be considered separately with respect to the faceted AF/F interface. The analysis of the influence of the AF/F interface plane was also the aim of the very first studies of Berkowitz and Greiner on Ni/NiO [16] and of van der Zaag et al. [27,28] on a series of [001] and [111] oriented epitaxial Fe_3O_4/CoO bilayers. The latter does not show opposite behavior for these two cases. Only few details on the structural characteristics of their samples and particularly the absence of the fine structure characterization of the AF/F interface do not allow them to clearly appreciate their magnetic results.

Figure 20 shows the evolution of the bias field as a function of the magnetite thickness at RT (dashed lines) and 20 K (solid lines) for the two main batches of bilayers for comparison. First comparison could be done on results obtained at room temperature. The $NiO/Fe_3O_4/Al_2O_3$(0001) system demonstrates a large bias field values at 300 K (250 Oe for the 10 nm thick Fe_3O_4 layer) whereas the one obtained on bilayers grown on MgO(001) is close to zero. The structural analyses have shown that the AF/F interface appears flat in the two systems but with a (111)-type plane in the NiO/(Ni,Fe)Fe_2O_4–Fe_3O_4/Al_2O_3(0001) system and a (001)-type for the bilayers grown on MgO(001). As presented in the experimental part, the NiO{001} planes are spin compensated surfaces while all the spins are parallel in the NiO{111} planes resulting in an uncompensated surface. Even with the appearance of a ferrimagnetic (Ni,Fe)Fe_2O_4 phase, only a weak NiO/(Ni,Fe)Fe_2O_4 interface roughness was evidenced by HRTEM (Fig. 6) and X-ray reflectivity measurements in bilayers grown on Al_2O_3. This indicates that the NiO(111) surface is almost flat and therefore one can assume to get rather large uncompensated NiO surfaces which is responsible for the shift of the magnetic loop at 300 K. Moreover the exchange field decreases with the inverse of the ferrimagnetic layer thickness as expected for an interfacial behaviour. Neglecting the thermal effects, a Meiklejohn-Bean model extended to a bilayers system with perfect uncompensated AF/F interface is expected to give a maximum value at zero temperature. In that model, the bias field is given by the expression:

$$H_B = \frac{nJ_{F/AF}\,|S_F|\,|S_{AF}|}{a^2 M_F t_F}$$

where $J_{F/AF}$ is the energy of an individual AF/F exchange bond at the interface (erg), S_i the spin of either F or AF layer, n/a^2 the number of exchange bonds by unit area, M_F the magnetisation of the F layer and t_F its thickness. We may calculate the extreme bias field at zero Kelvin using the magnetisation values measured in the single magnetite layers for different thickness and the estimated values given by the literature [43] for similar bonds in spinels $J_{F/AF} \approx 2.5 \times 10^{-15}$ erg making the assumption that it should be closed to the one of the real (Ni, Fe)Fe_2O_4/NiO interface With this approximate value we calculate a bias field 30 to 50 time larger than the value observed at 20 K. The discrepancy between this theoretical and experimental H_b values may also be due to the appearance of the mixing layer whose magnetization is less than the one of the pure magnetite and the lack of Ni atoms in the interface plane due to the interdiffusion and also interface roughness (i.e. a single atomic steps in the NiO(111) surface locally create anti-parallel spin alignment of the neighbouring flat interface terrace). At 300 K a strong decrease of the bias field is observed which points out the thermal effects and relaxation of the AF order due to small NiO crystalline anisotropy.

An increase of the coercive field of the F layer is generally associated to the AF/F exchange coupling. In all the models describing the AF/F exchange, the interface coupling restrains the motion of the magnetic domain boundaries and opposes the switching of the F layer. In these models, the coercive field is also expected to decrease with the inverse of the F thickness. The $1/t_F$ film thickness dependence of H_c is observed in the $NiO/Fe_3O_4/Al_2O_3(0001)$ system as reported in Figure 16 and underlines the interfacial origins of the effect. However we could observe that the H_c of our system, for $t_F = 20$ nm, is weaker than H_c of a simple Fe_3O_4 (20 nm) deposited on $Al_2O_3(0001)$. We could also notice that the coercive field of the thickest Fe_3O_4 layer (50 nm) does not reach the one expected for the bulk magnetite. Taking into account that the (Ni,Fe)Fe_2O_4 interphase exhibits a weaker coercive field and a weaker saturated moment and considering that the F layer is constituted by a 5–6 nm thick (Ni,Fe)Fe_2O_4 layer and the "pure" Fe_3O_4 film, the coercivity of our AF/F system is less than the one of the single pure Fe_3O_4 layer.

The exchange coupling of the AF/F bilayers grown on MgO appears drastically different, particularly at 300 K where the bias field is measured close to zero. The Fe_3O_4/NiO/MgO(001) epitaxial system demonstrates a high crystalline quality with flat compensated NiO(001) interface. In that case, the Malozemoff's model supposes that, because of the roughness inhomogeneities at the interface like atomic steps that cannot be avoid, the AF layer should break up into domains in order to minimise the energy (assuming the spin frustration at the interface). Calculation of the bias field shows an explicit link between the bias field and the domain wall energy of the AF which directly depends on the anisotropy constant K_{af}. The strength of K_{af} is also important to preserve the AF domains from switching when the F magnetisation is reversed during a magnetic loop. The weak intrinsic value of K_{af} for NiO (330 erg cm^{-3} at 300 K [44]) could explain such low bias. Therefore, the thermal energy and AF/F coupling are high enough to drag the NiO spins of the AF domains when the magnetisation of the adjoining Fe_3O_4 layer reverses. This justifies the absence of any significant bias at RT. Our system, characterized by an AF/F epitaxial interface, appears strongly different from some other polycrystalline AF/F systems [45,46] where anisotropy was developed in NiO/Co bilayers by NiO deposition at oblique incidence or under a convenient applied magnetic field.

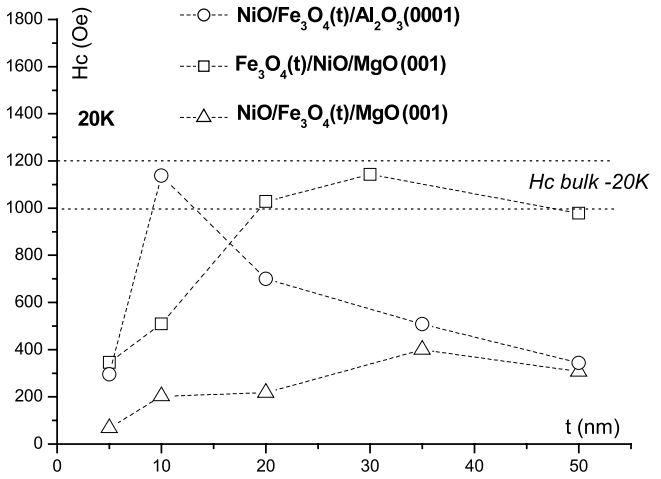

Fig. 21. Comparison between the variations of H_c at 20 K as a function of the magnetite thickness for (NiO/Fe_3O_4) bilayers grown on $Al_2O_3(0001)$ and (Fe_3O_4/NiO) and (NiO/Fe_3O_4) bilayers grown on MgO(001).

At 20 K the bias of Fe_3O_4/NiO/MgO(001) system is present and remains almost constant with the F thickness. These results are obtained at low temperature after a 5 T field cooling process. We must recall the analogous results of Borchers et al. [47] who observe an important biasing effect at low temperature in Fe_3O_4/NiO[001] superlattices. They measured at 80 K a bias field of 560 Oe and a coercive field of 1300 Oe after a 1.5 T field cooling from 325 K. These results are very close to what we observe in the Fe_3O_4/NiO/MgO(001) system. It suggests that the ferromagnetic order can be transmitted to the AF domains upon cooling from room temperature and that, at low temperature, the AF domains keep the memory of the state acquired during the field cooling process.

At 20 K, the H_c variations for the two bilayers grown on MgO(001) show a feature similar to what is observed for the bias field evolution (Fig. 21). The coercive field increases with the magnetite thickness to reach a constant value for the 35 nm thick magnetite layer. However, as for the NiO/Fe_3O_4 bilayer grown on $Al_2O_3(0001)$, the coercive field for the thickest magnetite layer of the NiO/Fe_3O_4/MgO(001) system does not reach the coercive field expected for the single magnetite layer of equivalent thickness. As already discussed, a Ni diffusion in the Fe_3O_4 layer was evidenced in NiO/Fe_3O_4 bilayers resulting in the growth of a nickel ferrite

interphase. H_c reaches almost the same value for the 50 nm thick ferrite layer in the $NiO/Fe_3O_4/MgO(001)$ and $NiO/Fe_3O_4/Al_2O_3(0001)$ systems (Fig. 21). On the contrary, in the $Fe_3O_4/NiO/MgO(001)$ system where no significant Ni diffusion is observed, the coercive field for the thickest magnetite layer reaches the value close to the one expected for the single Fe_3O_4 layer of equivalent thickness. This clearly confirms that the diffusion of Ni in the Fe_3O_4 layer for the two AF/F layers grown on MgO and $Al_2O_3(0001)$ which created a non stoechiometric nickel ferrite phase is responsible for the low value of the coercive field. Similar comments can be made on the magnetic measurements performed at RT. Only in the $Fe_3O_4/NiO/MgO(001)$ system with the thickest Fe_3O_4 layer (50 nm), H_c reaches the value measured in single layer of equivalent thickness: about 300 Oe at RT (see Fig. 18). In the two other stacking where the growth of a nickel ferrite phase has been evidenced, the H_c for the thickest ferrite layer is below 200 Oe (see Figs. 16 and 19).

6 Conclusion

The epitaxial growth of F/AF and AF/F bilayers composed by the ferrimagnetic Fe_3O_4 and the antiferromagnetic NiO oxides has been achieved on the two $Al_2O_3(0001)$ and MgO(001) substrates. Detailed structural analyses allow us to characterise the epitaxial structure and the quality of the interface for the two growth directions. When deposited on the first substrate, the epitaxial growth direction is [111] while it is [001] in the second case. These two growth directions have permitted the study of the influence of two drastically different types of AF/F interfaces on the exchange coupling: the first is constituted by the spin unbalanced NiO(111) surface and the second by the compensated NiO(001) surface. The exchange coupling is radically different for these two states. In the case of a NiO(111) interface, the bias and the coercive field decrease with the inverse of the ferrimagnetic layer thickness. This behaviour is the one expected considering an exchange coupling located at the interface as developed by most of the theoretical models. For a NiO(100) interface, the bias is almost zero at room temperature in agreement with a weak exchange coupling for such a spin compensated interface. At 20 K the bias and the coercive field exhibit the same unexplained dependence with the magnetite thickness: they first increase to reach a value that remains constant for ferromagnetic layers thicker than 50 nm (this result is probably correlated to the field cooled process, a larger study of this problem is in progress).

When NiO is deposited on the top of the Fe_3O_4 layer after an annealing step at 700 °C, an $(Ni,Fe)Fe_2O_4$ ferrite phase, isostructural with Fe_3O_4, is evidenced at the interface. The appearance of this ferrimagnetic phase whose coercive field and saturated magnetization is less than those of a pure Fe_3O_4 induces weaker H_c and saturated moment in the NiO/Fe_3O_4 bilayers than what is expected for a single magnetite layer.

The author would like to thank Dr. D. Hrabovsky (INSA Toulouse) for its kind help and fruitful discussions concerning the analysis of the magnetic data.

References

1. B. Dieny, J. Magn. Magn. Mater. **136**, 335 (1994)
2. C. Tsang, R.E. Fontana, T. Lin, D.H. Heim, V.S. Speriosu, B.A. Gurney, M.L. Williams, IEEE Trans. Magn. **30**, 3801 (1994)
3. W.C. Cain, W.H. Meiklejohn, M.H. Kryder, J. Appl. Phys. **61**, 4170 (1987)
4. J.S. Moodera, L.R. Kinder, T.M. Wong, R. Meservey, Phys. Rev. Lett. **74**, 3273 (1995)
5. See for example the web site of IBM Almaden Research Center: `http://www.almaden.ibm.com/sst/`
6. J.M. Daughton, Thin Solid Film **216**, 162 (1992); J.M. Daugthon, J. Appl. Phys. **81**, 3758 (1997)
7. W.H. Meiklejohn, C.P. Bean, Phys. Rev. **102**, 1413 (1956)
8. W.H. Meiklejohn, C.P. Bean, Phys. Rev. **105**, 904 (1957)
9. W.H. Meiklejohn, J. Appl. Phys. **29**, 454 (1958)
10. W.H. Meiklejohn, J. Appl. Phys. **33**, 1328 (1962)
11. J. Bransky, I. Bransky, A.A. Hirsch, J. Appl. Phys. **41**, 183 (1970)
12. C. Schlenker, R. Buder, Czech. J. Phys. B **21**, 506 (1971)
13. Y. Iwasaki, M. Takigushi, K. Bessho, J. Appl. Phys. **81**, 5021 (1997)
14. C. Schlenker, R. Buder, Phys. Stat. Sol. (a) **4**, K79 (1971)
15. A.E. Berkowitz, J.H. Greiner, J. Appl. Phys. **35**, 925 (1964)
16. A.E. Berkowitz, J.H. Greiner, J. Appl. Phys. **36**, 3330 (1965)
17. A.P. Malozemoff, Phys. Rev. B **35**, 3679 (1987)
18. A.P. Malozemoff, Phys. Rev. B **37**, 7673 (1988)
19. D. Mauri, H.C. Diegmann, P.S. Bagus, E. Kay, J. Appl. Phys. **62**, 1956 (1987)
20. N.C. Koon, Phys. Rev. Lett. **78**, 4865 (1997)
21. J. Nogués, I.K. Schuller, J. Magn. Magn. Mater. **192**, 203 (1999)
22. B. Dieny, V.S. Speriosu, S. Metin, S.S. Parkin, B.A. Gurney, P. Baumgart, D.R. Wilhoit, J. Appl. Phys. **69**, 4774 (1991)
23. T. Lim, C. Tsang, R.E. Fontana, J.K. Howard, IEEE Trans. Magn. **31**, 2585 (1995)
24. J.F. Bobo, S. Dubourg, E. Snoeck, B. Warot, P. Baules, J.C. Ousset, J. Magn. Magn. Mater. **206**, 118 (1999)
25. J. Nogués, D. Lederman, T.J. Moran, I.K. Schuller, K.V. Rao, Appl. Phys. Lett. **68**, 3186 (1996)
26. J. Nogués, D. Lederman, T.J. Moran, I.K. Schuller, Phys. Rev. Lett. **76**, 4624 (1996)
27. P.J. van der Zaag, R.M. Wolf, A.R. Ball, C. Bordel, L.F. Feiner, R. Jungblut, J. Magn. Magn. Mater. **148**, 346 (1995)
28. P.J. van der Zaag, A.R. Ball, L.F. Feiner, R.M. Wolf, P.A.A. van der Heilden, J. Appl. Phys. **79**, 5103 (1996)
29. Z. Zhang, S. Satpahi, Phys. Rev. B **44**, 13319 (1991)
30. S.A. Chambers, S.A. Joyce, Surf. Sci. **420**, 111 (1999)
31. J.M. Gaines, J.T. Kohlhepp, J.T.W.M.V. Eemeren, R.J.G. Elfrink, F. Roozeboom, W.J.M.D. Jonge, Mater. Res. Soc. Symp. Proc. **474**, 191 (1997)

32. D.S. Lind, S.D. Berry, G. Chern, H. Mathias, L.R. Testardi, Phys. Rev. B **4**, 1838 (1992)
33. Y.S. Dedkov, U. Rüdiger, G. Güntherodt, Phys. Rev. B **65**, 064417-1 (2002)
34. P. Seneor, A. Fert, J.-L. Maurice, F. Montaigne, F. Petroff, A. Vaures, Appl. Phys. Lett. **74**, 4017 (1999)
35. W. Eerenstein, T.T.M. Palstra, T. Hibma, S. Celotto, Phys. Rev. B **68,** 014428 (2003)
36. D.T. Margulies, F.T. Parker, F.E. Spada, R.S. Goldman, J. Li, R. Sinclair, A.E. Berkowitz, Phys. Rev. B **53**, 9175 (1996)
37. J.F. Bobo, D. Basso, E. Snoeck, C. Gatel, D. Hrabovsky, R. Mamy, S. Visnovsky, J. Hamrle, J. Teillet, A.R. Fert, Eur. Phys. J. B **24**, 43 (2001)
38. J.-B. Moussy, S. Gota, A. Bataille, M.-J. Guittet, M. Gautier-Soyer, F. Delille, B. Dieny, F. Ott, T.D. Doan, P. Warin, P. Bayle-Guillemaud, C. Gatel, E. Snoeck, to be published in Phys. Rev. B
39. A. Barbier, C. Mocuta, G. Renaud, Phys. Rev. B **62**, 16056 (2000)
40. B. Warot, E. Snoeck, P. Baulès, J.C. Ousset, M.J. Casanove, S. Dubourg, J.F. Bobo, Appl. Surf. Sci. **177**, 287 (2001)
41. B. Warot, E. Snoeck, P. Baulès, J.C. Ousset, M.J. Casanove, S. Dubourg, J.F. Bobo, J. Crystal Growth **234**, 704 (2002)
42. B. Warot, E. Snoeck, J.C. Ousset, M.J. Casanove, S. Dubourg, J.F. Bobo, Appl. Surf. Sci. **188**, 151 (2002)
43. A. Broese van Groenou, P.F. Bongers, A.L. Stuyts, Mater. Sci. Eng. **3**, 317 (1968/1969)
44. K. Kurosawa, M. Miura, S. Saito, J. Phys. C **13**, 1521 (1980)
45. M. Cartier, S. Auffret, P. Bayle-Guillemaud, F. Emult, F. Fettar, B. Dieny, J. Appl. Phys. **91**, 1436 (2002)
46. B. Diouf, L. Gabillet, A.R. Fert, D. Hrabovsky, V. Prochazka, E. Snoeck, J.F. Bobo, J. Magn. Magn. Mater. **265**, 204 (2003)
47. J.A. Borchers, Y. Ijiri, D.M. Lind, P.G. Ivanov, R.W. Erwin, S.H. Lee, C.F. Majkrzak, J. Appl. Phys. **85**, 5883 (1999)